

Extreme Low-Resolution Activity Recognition with Spatial-Temporal Attention Transfer

Yucai Bai Qiang Dai
Sichuan University

Long Chen*
Sun Yat-sen University

Lingxi Li Zhengming Ding
Indiana University-Purdue University Indianapolis

Qin Zou
Wuhan University

Abstract

Activity recognition on extreme low-resolution videos, e.g., a resolution of 12×16 pixels, plays a vital role in far-view surveillance and privacy-preserving multimedia analysis. Low-resolution videos only contain limited information. Given the fact that one same activity may be represented by videos in both high resolution (HR) and low resolution (LR), it is worth studying to utilize the relevant HR data to improve the LR activity recognition. In this work, we propose a novel Spatial-Temporal Attention Transfer (STAT) for LR activity recognition. STAT can acquire information from HR data by reducing the attention differences with a transfer-learning strategy. Experimental results on two well-known datasets, i.e., UCF101 and HMDB51, demonstrate that, the proposed method can effectively improve the accuracy of LR activity recognition, and achieves an accuracy of 58.12% on 12×16 videos in HMDB51, a state-of-the-art performance.

1. Introduction

In recent years, a large number of methods have been proposed for action recognition, and achieved considerable success, e.g., Two-Stream [21], C3D [22], and LRCN [6], etc. Most of these methods assume that, there is enough information in the region of raw pixels where the activities take place in image sequence. In such cases, action recognition models can well capture and represent the motions of the movement and classify the actions. However, this assumption does not always hold in practice due to the existing of low-resolution and low-quality videos. For instance, in the situation of far-view surveillance, there are often only few pixels for the targets (human in most cases) in the scene. Two examples are shown in the top row in Figure 1. For action recognition in such LR videos, cur-

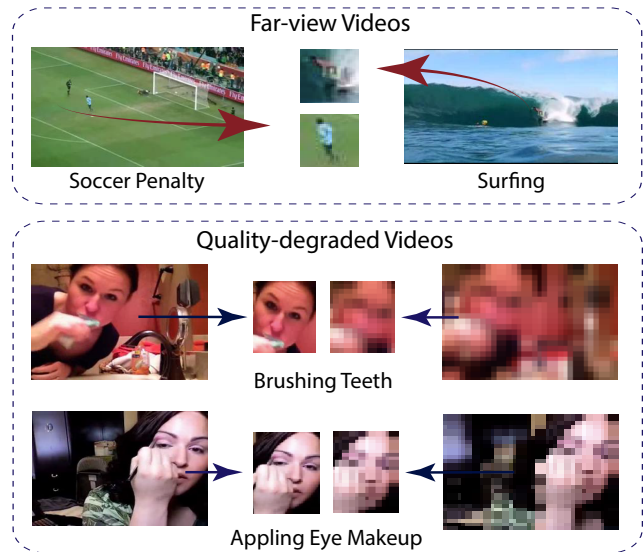


Figure 1. Activities in HR images and LR images. In far-view videos, activities can only be captured with very few pixels. In quality-degraded videos, activities are represented with blur LR images on a privacy-preserving purpose.

rent popular methods [21] [22] [6] cannot obtain acceptable accuracy.

Another situation that will generate LR videos is in privacy-preserving surveillance or data recording. With the advancement of mobile Internet and smartphones, videos can be easily captured and quickly spread. Meanwhile, average persons would have more concerns about the privacy preserving on the web. While videos are captured by ubiquitous cameras and stored in the cloud server, the concern is more urgent. Many technologies have been developed to deal with it, e.g., selective image blurring [2], obscuring [17], etc. In fact, a straightforward and effective way to address this problem is to directly collect LR data in the recording, which can also reduce the video-recording cost and the storage capacity. However, vision tasks on such LR

*The corresponding author is Long Chen (chenl46@mail.sysu.edu.cn)

videos may be limited. For example, the bottom of Figure 1 shows two images that are degraded for the privacy-preserving purpose. The face in the LR image is less than 25 pixels, which leads to a great challenge for face recognition.

The situation for action recognition is a little better since motion information can be extracted from image sequences. Many previous works [4] [26] [18] achieved considerable good results on 12×16 resolution videos, in detection of some specific actions. When the area corresponding to an activity is reduced to a few pixels, the part requiring attention will change. The amount of data in LR image, e.g., 12×16 , is about 0.2% of that in the original 256×340 images. With enough pixels, conventional algorithms can obtain low-level features by capturing geometry and texture details, and a large number of convolution operations and supervision signals from labels can be used to produce high-dimensional features. However, extremely LR data often do not have enough details for low-level features construction, which brings a bottleneck to the tradition.

How to extract effective information only from few pixels? An effective strategy is to explore the corresponding HR data. We make the assumption that, for a same action, the motion patterns in the LR videos have some relation with the motion patterns in the HR videos. The features of an action in the LR video may be clustered in one space, while features in the HR video may be clustered in another spaces. However, the distributions of these features in different space may be related using transfer learning. As such, action recognition in LR videos can benefit from the information of HR videos. Numerous previous researches [20] [19] [4] [18] [26] adopted this assumption for the higher recognition accuracy in LR video.

We also observe that, most of the existing methods for LR action recognition cannot achieve satisfactory accuracy for real-world applications. One possible reason is that they do not obtain the most useful information from few pixels and do not focus on the most informative area. The inessential areas seldom contain any vital clues for the recognition. In our strategy, these essential details could be obtained from the HR data. We focus on the more informative area, which can help do the recognition task. For example, the temporal intervals of swinging a golf club and the areas corresponding to the activity are more meaningful than others in determining whether it is an action of playing golf.

Based on the discussion above, we explore the spatial-temporal attention transfer model to help recognize actions at extremely low resolution in this paper. Specifically, we propose a novel knowledge transfer model to utilize more accurate signals from a powerful teacher network. The teacher network uses higher resolution image frames as input, and helps a student network to distinguish which frames are more effective and which parts are more informative for action recognition. We evaluate the proposed

method is evaluated on UCF101 and HMDB51, and achieve very promising results.

The contributions of this work are summarized as follows:

- A simple yet effective algorithm is proposed for measuring the spatial-temporal attention in LR videos. This algorithm is incorporated into the whole knowledge-transfer model for improving the LR action-recognition performance.
- A new strategy for dynamical weights adjusting is put forward, and an unsupervised method for data augmentation is presented to leverage various resolution supervisor signals.
- The proposed method is evaluated on several low-resolution activity benchmarks by comparing with the state-of-the-art methods. An accuracy of 58.12% is obtained on 12×16 HMDB51 videos.

2. Related Work

Action recognition has developed rapidly in recent years. Mainstream algorithms can be divided into mainly three categories. The first kind of algorithm is characterized by taking two streams as input and then estimating them jointly. In [21], RGB and optical flow data were used for prediction respectively, and then joint estimation was carried out. The second approach only uses the continuous RGB frames as input and 3D convolution to extract features to predict. C3D [22] used only a eight-layer neural network to achieve high precision. The subsequent R2PLUS1D [23] and P3D [16], factorizing the 3D convolutional enablers into separate spatial and temporal components, had achieved better results. The third type usually uses the recurrent neural network in the temporal dimension. LRCN [6] constructed a recurrent sequence model, which is directly connected to the new visual convolutional network. In our proposed method, we use RESNET-34 [8] and R2PLUS1D [23] as feature extraction backbones.

Teacher-student learning, as one of the distillation methods, has also been used in recent years. Typically, the teacher network has a better performance or more abundant data, which can help student network to grasp the key features better. For example, [7] used teacher network to help student network with faster inference speed but poorer performance to select training data to enhance accuracy. In speech recognition, [14] proposed a condition-robust unsupervised domain adaptation method, which uses this novel learning paradigm for unsupervised learning. [1] proposed a more intensive teacher-student network by using sparse picture frames as input. However, in the field of LR action recognition, there is no related practice.

There are also some related achievements in the field of LR recognition. [25] put forward this problem first, then tried several conventional methods and developed an improved model for this problem. [12] used the shared network to identify diverse resolution data respectively and then reduced the differences in the mimic layer to improve the accuracy further. [11] expanded the LR image to a higher quality one through deconvolution to better recognize human faces. In the field of LR action recognition, [4] proposed a semi-coupled, later-sharing network, which makes student network have more accurate weights by sharing part of the weights of both the teacher network and the student network. [18] used the embedding technique of different downsampling methods, which uses to make the network embed this map to its weights. [15] applied the self-attention technique and learn the soft targets encoded by teacher work, rather than learning more effective attention as we did. However, these methods do not focus on the informative area, which is one of the reasons they can not achieve satisfactory accuracy.

3. The Approach

In this section, we describe our proposed methods to recognize multi-class actions from low-resolution videos in details. Specifically, we first introduce the acquisition of attention from a single model, which illustrates how to capture the distribution of attention in the abundant data. Then, we describe the spatial-temporal attention transfer process, where the powerful model imparts more effective attention to the weaker counterpart as a supervision signal. Finally, we present some strategies in the training stage to solve the over-fitting and help the network learn easier from multiple monitoring signals.

3.1. Attention Acquisition

The premise of attention transfer is to obtain the attention of the network at first. Attention is obtained from two aspects, spatial dimension and temporal dimension. Spatial attention refers to the spatial area from which the model classifies the action, might contain the human and corresponding paraphernalia, such as golf club or soccer. Attention in the temporal dimension refers to the keyframes containing important action feature in the whole videos.

Our method are based on the assumption, which is the numerical value of the output represents the degree of attention of the network. The weights in the network and the output of each layer ultimately lead to the final result.

3.1.1 Spatial Attention Definition

The output of each intermediate layer holds the clue of 2D spatial relationships. What we need to do is to construct a mapping from the 3D output to a 2D positional relationship.

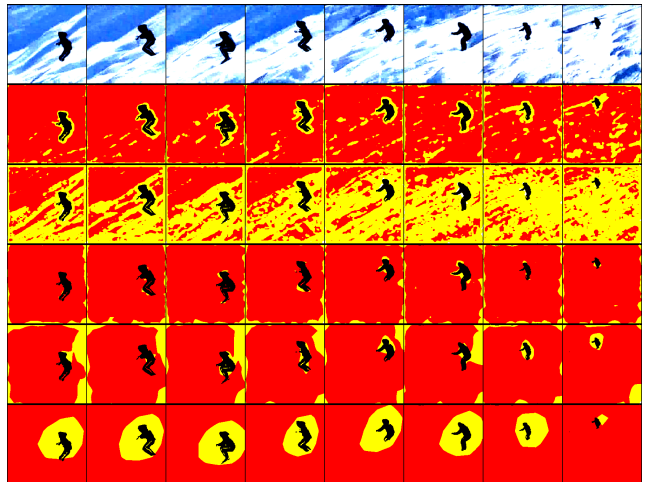


Figure 2. Visualization of the spatial attention in the "skiing" category. Yellow and red represent greater and less attention, respectively. The first row is the original input, and the following rows are the attention results from each RESNET block.

The three-dimensional output is $H \times W \times C$, which represents C feature planes with spatial dimensions $H \times W$. The patterns captured by different channels vary based on different details. However, there are always features of specific areas included in a large number of channels. Based on the feature of the above 3D tensor, we put all the values of the channels together for consideration. More specifically, we define the following activation-based spatial attention map:

$$F_{x,y}(O) = \sum_{i=1}^C |O_{x,y,i}| \quad (1)$$

where O means the 3D output of network and x, y, i represents the specific position of the output. The visualization of spatial attention is shown in Figure 2.

3.1.2 Temporal Attention Definition

In order to distinguish the importance of different time segments, we divide a whole video into K segments (In our experiment section, we set $K = 4$ and 8). We use the segment as the basic unit and sample one or some consecutive frames from it as the input of the model. After the independent classification, we finally perform video-level prediction on all the results of K segments.

In order to capture the importance of each interval, different from TSN [24], we specially designed a temporal attention module (TAM) to estimate corresponding importance, as shown in Figure 3. Specifically, we use the feature of each interval as input and stack all features together to perform two fully-connected layers, 64-dimensional and K -dimensional, respectively.

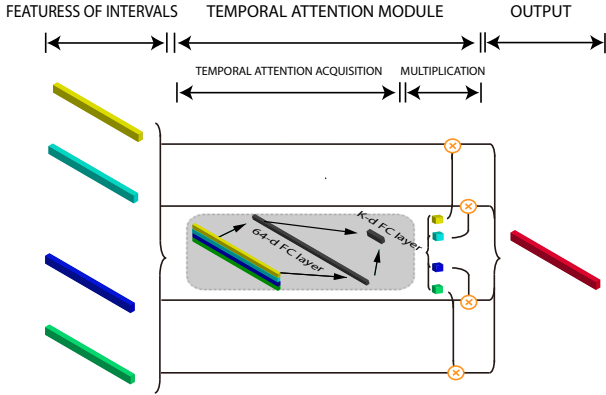


Figure 3. Temporal Attention Module. Features of each interval are put together to generate their respective attention values, which are then multiplied by the original features to produce the final result.

The model takes the results of the feature extraction module as input, processes data through two fully-connected (FC) layers, and finally normalizes the data results to $[0,1]$ interval through a softmax layer. The output is assumed as the importance of each time segment, which is multiplied by the corresponding features to get the final video-level result.

3.1.3 Training Setting

A general backbone is needed to extract features from the input data. In our experiment section, we used both the light 2D convolution and the more powerful 3D convolution. RESNET-34 was used as a 2D convolution network, which only has $3.6 * 10^9$ FLOPs. Therefore, we could run more intervals at the same time in a limited memory. For the higher accuracy requirement, we also used a slow yet powerful R2PLUS1D model. Its strong performance benefits from its novel structure replacing the 3D convolutional filters size $N \times t \times d \times d$ with a (2+1)D RESNET block consisting of M spatial 2D filters of size $N \times 1 \times d \times d$ and N temporal convolutional filters of size $M \times t \times 1 \times 1$.

We use stochastic gradient descent as our loss optimization method. The pertained weight from IMAGENET [5] or KINETICS [10] is also used as our initialization weight to accelerate our convergence process. For a better convergence, we also use Batch Normalization(BN), which estimates the activation mean and variance within each batch and uses them to transform these activation values into a standard Gaussian distribution. For reducing computing cost, our network freezes the BN layer expect the first layer and uses clip gradient.

3.2. Attention Transfer

We use two networks, teacher network (T-Net) and student network (S-Net), and adopt the teacher-student learning (TS Learning) to implement the training process. Besides, we propose a Spatial-Temporal Attention Transfer (STAT) loss to capture the gap in attention between the two networks.

3.2.1 Teacher-Student Learning (TS Learning)

We construct the same network of teachers and students with different resolution as input. More specifically, we input the HR data (256×340) into the T-Net and the LR data (12×16) which are sampled from the HR data into S-Net. By continuously forcing the intermediate processing output of the two networks, spatial attention and temporal attention, students can better grasp what the network should pay attention to. The learning process is shown in Figure 4.

3.2.2 Spatial-Temporal Attention Transfer Loss

The proposed STAT loss is composed of the spatial attention loss, temporal attention loss and cross-entropy loss.

For computing spatial attention loss, we obtain both spatial attention from T-Net and S-Net firstly. Then, we minimize the output of the same index layer of the two networks to reduce the spatial attention difference. T-Net with the more supervisory signal and better performance is more sensitive to the same action, so that the area that T-net pays more attention is more likely to be the key information of action judgment. The network can notice the key parts better that lead to a higher performance.

However, the parameters of T-Net, supervision signal for the S-Net, are very complex. If all weights are used as supervisory signals, the whole network will run slowly when calculating losses. Besides, the T-Net must have parameters that deal with its own features, which may interfere with the TS learning. So we need to pick the most representative output. In our experiments, we choose each RESNET block output as attention. To make the difference more obvious, we square the subtracted data in the spatial dimension. Let S , T , and W^S , W^T denote student, teacher and their weights respectively. Let also Res denote the RESNET block outputs pairs of both networks for which we want to transfer attention maps. Then we can define the following SAT(Spatial Attention Transfer) loss:

$$L_{SAT} = \sum_{i \in Res} \left\| \frac{Q_S^i}{\|Q_S^i\|_2} - \frac{Q_T^i}{\|Q_T^i\|_2} \right\|_P \quad (2)$$

where $Q_S^i = vec(F(A_S^i))$ and $Q_T^i = vec(F(A_T^i))$ are the i -th pair of student and teacher attention maps in vectorized

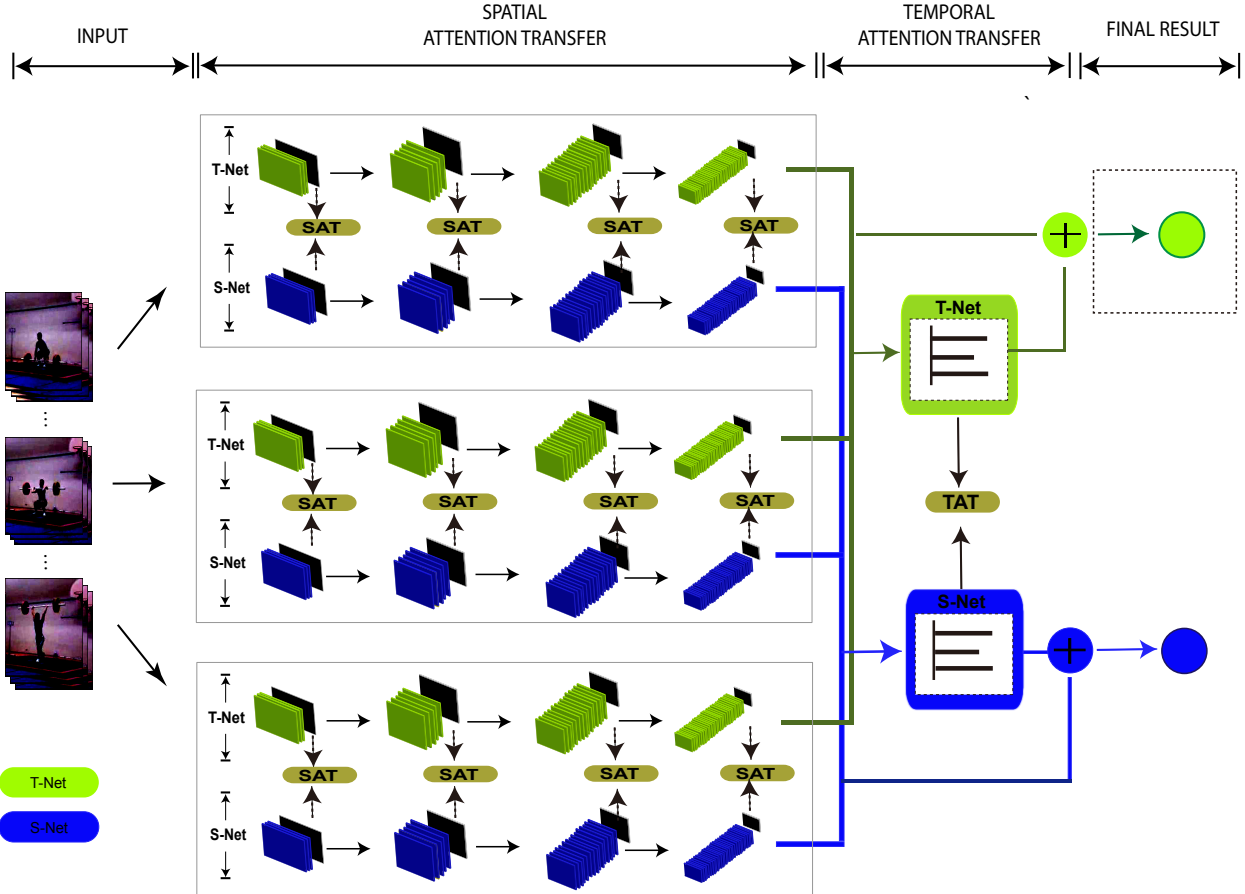


Figure 4. Overview of spatial-temporal attention transfer. Given an K segments extracted from a video (K is 3 in the figure), T-Net and S-Net generate spatial attention and time attention values simultaneously. The proposed STAT loss is used to force the attention difference reduce.

form, respectively, and P refers to norm type (in the experiments we use $P = 2$).

For temporary attention loss, we focus on the discrepancy between the output of two TAM, which is designed for observing the role of different time zones in the final result easily. So we can concentrate on the period with more precise behaviour information. In this loss function, we subtract the output from the two TAM, so as to force S-Net to pay more attention to the importance interval, which is easy to judge the action category. Besides the final FC layer, we also designed a 64-dimensional hidden layer to magnify the differences in intermediate processing. In order to make the difference more significant, we use the same method as spatial attention loss and use the square method to deal with the difference. We define the following TAT(Temporal Attention Transfer) loss as:

$$L_{TAT} = \sum_{j \in fc} \left\| \frac{Q_S^j}{\|Q_S^j\|_2} - \frac{Q_T^j}{\|Q_T^j\|_2} \right\|_P \quad (3)$$

where fc denotes the FC layer outputs pairs in temporal attention module.

Finally, in addition to the two loss functions mentioned above, we also add cross-entropy loss (CE) to help the network be sensitive to the final results. Cross-Entropy is often used as a loss function for classification problems. Its value represents the difference between the final output and the label in video-level prediction. We define the total loss as:

$$L_{total} = W_{CE} \times L_{CE} + W_{SAT} \times L_{SAT} + W_{TAT} \times L_{TAT} \quad (4)$$

where W_{CE} , W_{SAT} , W_{TAT} are the weight of cross-entropy loss, the weight of spatial attention loss, and the weight of temporal attention loss, respectively.

3.3. Training Strategies

In the training stage, there are two challenges. One is the over-fitting due to the insufficient labelled data. Another

problem is the contradiction between the importance of the supervisory signal and the difficulty of training. Specifically, the deeper output is crucial for final prediction but hard to learn because that is based on the output of shallower layers.

3.3.1 Unsupervised Training Method

Compared to single-frame pictures, video analysis application requires more data to conclude the temporal information. Moreover, the LR model can not directly utilize existing pre-training weights because of its different low-level features from existing common datasets. We have no choice but to collect more data to train the network. However, labelling video data manually is an extremely tedious task.

In our training, we use an unsupervised approach to meet the huge demand for data. That is using the fixed-parameter T-Net to encode data as the soft label. There are certain requirements for training data; that is, the main body of action is human and contains a complete action rather than cut-off video. Under such requirements, the most easily available datasets are the raw video of SPORTS-1M [9] and KINETICS [3], which not contains manually annotating information. In our unsupervised training, we only use SAT and TAT in the loss function. We use this unsupervised training method before the formal training to use extra data to overcome the over-fitting.

3.3.2 Rolling Weights

How to solve the contradiction between training difficulty and its importance? We consider that the key to solve this problem is adopting different training strategies in different stages. When we use a certain proportion in our experiments, 10%-20%-30%-40% in spatial part and 33%-66% in temporal part, the final result is unsatisfactory. The reason for the undesirable result is that the deeper layer, which accounts for a large proportion, has a large gap between the two networks and hard to learn. It is necessary to modify the weights of the shallower layer rather than the weights of the deeper layer itself because deep information is based on the shallow part of the networks due to the different resolution. The features that need to be extracted from the shallow layers of the two networks are not very close. To solve this problem, we propose a training method to update the weights, that is, the ratio of different parts changes with the training. Specifically, we alternately use (40%, 30%, 20%, 10%), (30%, 40%, 20%, 10%), (20%, 30%, 40%, 10%), and (10%, 20%, 30%, 40%) in spatial part and alternately use (66%, 33%) and (33%, 66%) in temporal part in every 10 epochs. The purpose is to enable the network to learn the weight better behind.

4. Experiments

In this section, we evaluate and report the results of the proposed method of action recognition on extremely low-resolution videos.

4.1. Dataset and Setting

We use the common dataset for multi-class action classification, e.g. UCF101 and HMDB51, and the down-sampling is taken.

HMDB dataset is one of the most famous public datasets for action classification, which contains more than 7000 videos with 51 different action categories. The dataset is composed of the videos mostly collected from YouTube, including movie scenes. We resized the HMDB videos to 12×16 using the average downsampling, while also include the lens blur term and the Gaussian noise term. For the videos with non-3:4 aspect ratio, a centre cropping was used. The standard evaluation setting of the dataset using 3 provided training/testing splits was followed, performing the 51-class video classification.

The UCF101 dataset contains 101 classes and 13320 video clips. We follow the evaluation scheme of the THUMOS13 challenge and adopt the three training/testing splits for evaluation. Each split in UCF101 includes about 9.5K training and 3.7K test videos. For a more natural comparison, we used the same down-sampling strategy as HMDB51, including the resize resolution and centre crop. The low-resolution UCF101 has never been used in other LR action recognition methods before because the size of the people in the dataset is so small that it is difficult to identify them compared to HMDB51. After considering this reason, we still choose this dataset because we can achieve a sufficient accuracy in HR data. (our prec@1 can reach 90.56% using R2PLUS1D-18 on UCF101, and the same structure can only reach 62% of prec@1 on HMDB51). T-Net accuracy plays a crucial role in teacher-student architecture.

4.2. Implementation Details

In our experiments, we used two backbones as the feature extraction module, RESNET-34(2D) and R2PLUS1D(3D) for different reasons. In the network represented by RESNET-34 with the 2D image as input, the memory usage is small, which means that the video of the same duration can be divided into more intervals in a limited memory. In this way, the interval can contain more precise information, and temporal attention information is more accurately transmitted to S-Net. For the R2PLUS1D, it uses continuous RGB frames as input, which usually takes up more video memory, but it can handle complex information better. In our practice, the input for RESNET-34 is a single-frame image, and the whole video is divided into eight in-

Table 1. The results on 12×16 UCF101 dataset using RESNET-34 for different weights. The first four rows are fixed weight, and the last row is the rolling weight. The term Overall, SAT, TAT denote CE-SAT-TAT, Res1-Res2-Res3-Res4 (the output from each RESNET block), FC1-FC2(the output in temporal attention module), respectively.

Weight Type	Overall	SAT	TAT	Prec@1
Fixed	1/7 - 4/7 -2/7	1/4-1/4-1/4-1/4	1/2-1/2	45.70%
Fixed	4/7 - 1/7 -2/7	1/15-2/15-4/15-8/15	1/3-2/3	44.96%
Fixed	1/3 - 1/3 -1/3	1/4-1/4-1/4-1/4	1/2-1/2	46.60%
Fixed	1/3 - 1/3 -1/3	1/15-2/15-4/15-8/15	1/3-2/3	46.15%
Fixed	1/3 - 1/3 -1/3	0-0-0-1	0-1	45.78%
Rolling	-	-	-	46.90%

tervals. For R2PLUS1D-18, the input from four intervals containing five consecutive frames each.

Our entire training process is as follows: First, a single model training is conducted, including T-Net with HR data as input and S-Net with LR data as input, then a teacher-student model joint training is performed. In the single model training process, we use the mini-batch SGD to learn the network parameters, and the batch size is set to 256 and momentum is set to 0.9. The initial learning rate is 0.001, and the learning rate is divided by 10 for every 20 epochs. The first five epochs use the warm-up technique to find the direction of the gradient descent better. A total of 50 epochs were performed. Only cross-entropy was used as the loss function. We use the techniques of location jittering, horizontal flipping, cropping, and scale jittering for data augmentation.

TS leaning is trained in the second stage. The weight of the three parts has a significant effect on the final result. We conducted related experiments on the above problems, and the experimental results are shown in Table 1. We can see that, for the fixed weight, the best results are obtained when CE, SAT, and TAT are both 1/3. This can indicate that both SAT and TAT play a supporting role for the final result. For the weights in the middle of the SAT, the accuracy of the gradually-increase weight (1/15-2/15-4/15-8/15) is lower than the equal weight (1/4-1/4-1/4-1/4) of the weight at different overall weights, which shows that the weight setting directly according to the importance of the final result does not achieve the best. The reason is the deep processing depends on the output of the shallow network. TAT weight setting is the same as the SAT. The rolling weight exceeds all the fixed weights because the contradiction between the importance of different weights and the dependence of adjacent weights is partly solved.

4.3. Visualization of Spatial-Temporal Attention

In this subsection, we visualize the spatial attention and temporal attention in the inference. In order to have more segments and make the effect of the temporal attention module more prominent, we used less-memory required RESNET-34 as the backbone. In the spatial attention visu-

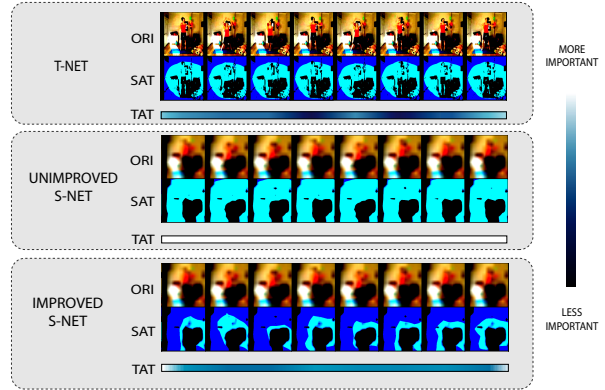


Figure 5. This figure consists of three parts. From top to bottom, T-Net results, unimproved S-Net results, and the improved S-Net are shown. The first row is the original image, the second row is the visualization of spatial attention of last RESNET block, and the bar in the bottom is the visualization of temporal attention.

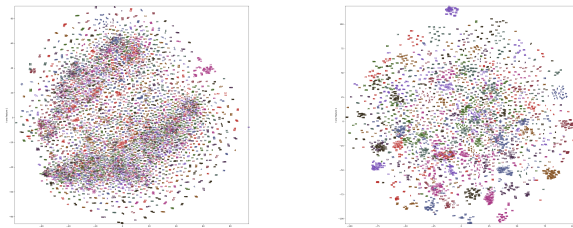


Figure 6. Video representation embedding visualizations of unimproved S-Net and improved S-Net on UCF101 using t-SNE. Each item is visualized as one point and colors denote different actions.

alization, we randomly sample one frame from corresponding intervals as input. Then the input goes through four RESNET blocks. We perform the average operation on the output of each RESNET block in the channel dimension. Then the result is resized to the shape of the input by the bilinear interpolation, and we multiply it by the original image. In the temporal attention visualization, we put 512-dimensional features of each interval into the FC layers. Finally, the attention value for each interval is generated. We colored the temporal attention value in the bottom bar.

As shown in Figure 5, we can identify that, the action is jumping. In the result of T-Net, the spatial attention is around the human, and the improved S-Net also obtains the information. However, the original algorithm focuses on the whole input. For temporal attention, the unimproved models can not capture the key segments, which play a vital role in the final classification.

Table 2. The results on different resolution UCF101 dataset with our spatial-temporal attention transfer are shown.

Resolution	Before Prec@1	Before prec@5	After Prec@1	After Prec@5
(6 × 8)	32.24	53.76	36.43	56.43
(12 × 16)	42.79	67.64	46.66	67.75
(18 × 24)	51.28	73.12	53.07	75.69
(24 × 32)	54.53	79.06	55.65	79.54

4.4. Visualization of Video Representation Embedding

Figure 6 further shows the t-SNE [13] visualization of embedding of video representation learnt by original model and improved model. More specifically, we randomly select 9K videos from UCF101 and the video-level representation is then projected into two-dimensional space using t-SNE. Our method aiming at focusing on the more informative part is better semantically separated than the original one.

4.5. Comparison at Different Resolutions

Even though most of the relevant experiments are based on 12 × 16 resolution, we still believe that experiments at multiple resolutions are necessary. For two reasons, more resolution comparison experiments are beneficial for balancing trade-off issues with resolution and accuracy, in practice. Another reason is that we prove that our method is valid at all different resolutions.

As shown in Table 2, our method works at different resolutions, and the accuracy gradually decreases with increasing resolution. The increase in prec@1 is 4.19%, 3.87%, 1.79%, and 1.12%, respectively. The improvement of prec@5 is much smaller, from 2.67% to 0.48%. As the resolution increases, the accuracy of action recognition and spatial-temporal attention are more accurate. Therefore, the effect of TS learning decreases.

4.6. Exploration Study

In this subsection, we focus on our proposed learning methods and its best practices. In this experiment, we used two backbones, RESNET-34 and R2PLUS1D-18, respectively. We only used RGB images as input in this experiment. We did the relevant experiments to get the best practices. We used the 0.5-0.5-0, 0.5-0-0.5, 0.33-0.33-0.33 to represent SAT, TAT, SAT+TAT respectively. In addition, we used the training strategy of rolling weight to make the weights easier to learn. Unsupervised learning is also added to the training because it avoids over-fitting.

As can be seen in Table 3, the performance is increased by 5.37% and 5.97%, respectively, under RESNET-34 and R2PLUS1D-18, after applying our proposed method. The latter is better than the former because T-Net has a higher accuracy (78.82% in RESNET-34, 90.56% in R2PLUS1D-

Table 3. The results on the 12 × 16 UCF101 dataset with our spatial-temporal attention transfer. The student row is the baseline of the entire experiment. We used the SAT, TAT and SAT+TAT, respectively. Besides we use *rc* and *ut* present the rollings weights and unsupervised training method, respectively.

	RESNET-34	R2PLUS1D-18
Teacher	78.82%	90.56%
Student	42.79%	48.95%
SAT	45.76%	52.03%
TAT	44.97%	50.59%
SAT+TAT	46.66%	52.34%
SAT+TAT+ <i>rc</i>	46.85%	53.21%
SAT+TAT+ <i>rc</i> + <i>ut</i>	48.03%	54.92%

18), which can provide more information. For the same reason, the latter network is also relatively stronger with LR data than the former one. After applying our proposed spatial and temporal attention loss function, the accuracy has been improved obviously on each network, from 42.79% to 46.66% on RESNET-34 and from 48.95% to 52.34% on R2PLUS1D-18. It is worth noting that the TAT module has a smaller boost on R2PLUS1D-18 than on RESNET-34. This is because of the different amount of intervals, and RESNET-34 can have a more precise range for sampling frames. The proposed rolling weight to solve the contradiction between the importance of different weights and the dependence of adjacent weights also helps with accuracy in both networks. Finally, unsupervised learning partially solved the problem of over-fitting by adding unlabeled data, which has been increased by 1.13% in RESNET-34 and 1.71% in R2PLUS1D-18, respectively.

4.7. Comparison with the State-of-the-Art

After assembling all the techniques described, we test it on the challenging datasets: 12 × 16 HMDB51. The results are summarized in Table 4. It is not difficult to observe that our results outperform all state-of-the-art approaches on LR action classification. For the fairness of comparison, we used the same experimental setting as [15], which is 64 frames of the optical stream and RGB images were used as input, and we used R2PLUS1D-34 as our backbone, the performance of which is close to I3D.

5. Conclusion

In this paper, we used spatial-temporal attention transfer to help student network to improve accuracy in LR data. The accuracy of our approach achieved the state-of-the-art level, 58.12% on 12 × 16 HMDB51. This is primarily due to the more precise spatial-temporal attention, which is provided by teacher network. The unsupervised learning for data augmentation and the learning strategy of the rolling weights significantly improved the final accuracy.

Table 4. Performance of our model compared to the state-of-the-art results on the 12×16 HMDB51 dataset. R2PLUS1D-34 is used as the backbone.

Approach	Accuracy
PoT [20] (CVPR'15)	26.57%
ISR [19] (AAAI'17)	28.68%
Simonyan, et al [4] (WACV'17)	29.20%
Ryoo, et al [18] (AAAI'18)	37.70%
Xu, et al [26] (WACV'18)	44.96%
I3D [3] (CVPR'17)	52.61%
Didik, et al (I3D) [15] (ICCVW'19)	57.84 %
R2PLUS1D-34 [23] (CVPR'18)	52.29%
Ours(R2PLUS1D-34)	58.12%

References

- [1] Shweta Bhardwaj, Mukundhan Srinivasan, and Mitesh M Khapra. Efficient video classification using fewer frames. In *Proceedings of the IEEE Conference on Computer Vision and Pattern Recognition*, pages 354–363, 2019.
- [2] Michael Boyle, Christopher Edwards, and Saul Greenberg. The effects of filtered video on awareness and privacy. In *Proceedings of the 2000 ACM conference on Computer supported cooperative work*, pages 1–10. ACM, 2000.
- [3] Joao Carreira and Andrew Zisserman. Quo vadis, action recognition? a new model and the kinetics dataset. In *The IEEE Conference on Computer Vision and Pattern Recognition (CVPR)*, July 2017.
- [4] Jiawei Chen, Jonathan Wu, Janusz Konrad, and Prakash Ishwar. Semi-coupled two-stream fusion convnets for action recognition at extremely low resolutions. In *2017 IEEE Winter Conference on Applications of Computer Vision (WACV)*, pages 139–147. IEEE, 2017.
- [5] J. Deng, W. Dong, R. Socher, L.-J. Li, K. Li, and L. Fei-Fei. ImageNet: A Large-Scale Hierarchical Image Database. In *CVPR09*, 2009.
- [6] Jeffrey Donahue, Lisa Anne Hendricks, Sergio Guadarrama, Marcus Rohrbach, Subhashini Venugopalan, Kate Saenko, and Trevor Darrell. Long-term recurrent convolutional networks for visual recognition and description. In *Proceedings of the IEEE conference on computer vision and pattern recognition*, pages 2625–2634, 2015.
- [7] Shiming Ge, Shengwei Zhao, Chenyu Li, and Jia Li. Low-resolution face recognition in the wild via selective knowledge distillation. *IEEE Transactions on Image Processing*, 28(4):2051–2062, 2018.
- [8] Kaiming He, Xiangyu Zhang, Shaoqing Ren, and Jian Sun. Deep residual learning for image recognition. In *Proceedings of the IEEE conference on computer vision and pattern recognition*, pages 770–778, 2016.
- [9] Andrej Karpathy, George Toderici, Sanketh Shetty, Thomas Leung, Rahul Sukthankar, and Li Fei-Fei. Large-scale video classification with convolutional neural networks. In *Proceedings of the IEEE conference on Computer Vision and Pattern Recognition*, pages 1725–1732, 2014.
- [10] Will Kay, Joao Carreira, Karen Simonyan, Brian Zhang, Chloe Hillier, Sudheendra Vijayanarasimhan, Fabio Viola, Tim Green, Trevor Back, Paul Natsev, et al. The kinetics human action video dataset. *arXiv preprint arXiv:1705.06950*, 2017.
- [11] Pei Li, Loreto Prieto, Domingo Mery, and Patrick J Flynn. On low-resolution face recognition in the wild: Comparisons and new techniques. *IEEE Transactions on Information Forensics and Security*, 14(8):2000–2012, 2019.
- [12] Ze Lu, Xudong Jiang, and Alex Kot. Deep coupled resnet for low-resolution face recognition. *IEEE Signal Processing Letters*, 25(4):526–530, 2018.
- [13] Laurens van der Maaten and Geoffrey Hinton. Visualizing data using t-sne. *Journal of machine learning research*, 9(Nov):2579–2605, 2008.
- [14] Zhong Meng, Jinyu Li, Yifan Gong, and Bing-Hwang Juang. Adversarial teacher-student learning for unsupervised domain adaptation. In *2018 IEEE International Conference on Acoustics, Speech and Signal Processing (ICASSP)*, pages 5949–5953. IEEE, 2018.
- [15] Didik Purwanto, Rizard Renanda Adhi Pramono, Yie-Tarnng Chen, and Wen-Hsien Fang. Extreme low resolution action recognition with spatial-temporal multi-head self-attention and knowledge distillation. In *The IEEE International Conference on Computer Vision (ICCV) Workshops*, Oct 2019.
- [16] Zhaofan Qiu, Ting Yao, and Tao Mei. Learning spatio-temporal representation with pseudo-3d residual networks. In *proceedings of the IEEE International Conference on Computer Vision*, pages 5533–5541, 2017.
- [17] Nisarg Raval, Animesh Srivastava, Kiron Lebeck, Landon Cox, and Ashwin Machanavajjhala. Markit: Privacy markers for protecting visual secrets. In *Proceedings of the 2014 ACM International Joint Conference on Pervasive and Ubiquitous Computing: Adjunct Publication*, pages 1289–1295. ACM, 2014.
- [18] Michael S Ryoo, Kiyoon Kim, and Hyun Jong Yang. Extreme low resolution activity recognition with multi-siamese embedding learning. In *Thirty-Second AAAI Conference on Artificial Intelligence*, 2018.
- [19] Michael S Ryoo, Brandon Rothrock, Charles Fleming, and Hyun Jong Yang. Privacy-preserving human activity recognition from extreme low resolution. In *Thirty-First AAAI Conference on Artificial Intelligence*, 2017.
- [20] Michael S Ryoo, Brandon Rothrock, and Larry Matthies. Pooled motion features for first-person videos, 2015.
- [21] Karen Simonyan and Andrew Zisserman. Two-stream convolutional networks for action recognition in videos. In *Advances in neural information processing systems*, pages 568–576, 2014.
- [22] Du Tran, Lubomir Bourdev, Rob Fergus, Lorenzo Torresani, and Manohar Paluri. Learning spatiotemporal features with 3d convolutional networks. In *Proceedings of the IEEE international conference on computer vision*, pages 4489–4497, 2015.
- [23] Du Tran, Heng Wang, Lorenzo Torresani, Jamie Ray, Yann LeCun, and Manohar Paluri. A closer look at spatiotemporal convolutions for action recognition. In *Proceedings of the IEEE conference on Computer Vision and Pattern Recognition*, pages 6450–6459, 2018.

- [24] Limin Wang, Yuanjun Xiong, Zhe Wang, Yu Qiao, Dahua Lin, Xiaoou Tang, and Luc Van Gool. Temporal segment networks: Towards good practices for deep action recognition. In *European conference on computer vision*, pages 20–36. Springer, 2016.
- [25] Zhangyang Wang, Shiyu Chang, Yingzhen Yang, Ding Liu, and Thomas S Huang. Studying very low resolution recognition using deep networks. In *Proceedings of the IEEE Conference on Computer Vision and Pattern Recognition*, pages 4792–4800, 2016.
- [26] Mingze Xu, Aidean Sharghi, Xin Chen, and David J Crandall. Fully-coupled two-stream spatiotemporal networks for extremely low resolution action recognition. In *2018 IEEE Winter Conference on Applications of Computer Vision (WACV)*, pages 1607–1615. IEEE, 2018.